Advanced Sciences and Technology Journal

ASTJ vol. 2 no.3 (2025) P1080
10.21608/ASTJ.2025.397523.1080
https://astj.journals.ekb.eg/

Application of Machine Learning in Predicting Heavy Metal Uptake by Activated Carbon Adsorbents

Merna El Shafie[1, *], Mahmoud F. Mubarak [2], Mahmoud Nasr[3], Amina Shaltout[4], Abeer El Shahawy[4]

[1]*Civil Engineering Department, Higher Institute of Engineering and Technology, Fifth Settlement*

[2]*Petroleum Applications Department, Egyptian Petroleum Research Institute (EPRI),1 Ahmed El Zomor St. Nasr City, Cairo, 11727, Egypt*

[3]*Sanitary Engineering Department, Faculty of Engineering, Alexandria University, Alexandria, 21544, Egypt*

[4]*Department of Civil Engineering, Faculty of Engineering, Suez Canal University, PO Box 41522, Ismailia, Egypt*
**merna.ahmed@et5.edu.eg*

ARTICLEINFO

Article history:
Received 24 June 2025
Revised 22 July 2025
Accepted 23 July 2025
Available online 26 September 2025
Special Issue (AIDS 2025)
Handling Editor:
Prof. Dr. Mohamed Talaat Moustafa

Keywords:
Machine learning
Activated carbon
Heavy metal removal
Adsorption
Artificial neural network

ABSTRACT

The contamination of water resources by transition metals such as manganese (Mn^{2+}), cobalt (Co^{2+}), and copper (Cu^{2+}) poses significant environmental and health concerns, necessitating the development of sustainable treatment solutions. This study explores the use of activated carbon derived from reed biomass as a low-cost, eco-friendly adsorbent for metal removal. An Artificial Neural Network (ANN) model was developed using a dataset of 435 experimental entries and trained on seven input variables: solution pH, contact time, initial ion concentration, adsorbent dosage, specific surface area (SSA), point of zero charge (pHpzc), and surface functional group intensity (SFG). The ANN optimized using the Levenberg–Marquardt algorithm with one hidden layer of eight neurons, demonstrated high predictive accuracy, achieving R^2 values of 0.949 (Mn^{2+}), 0.948 (Co^{2+}), and 0.923 (Cu^{2+}). Sensitivity analysis indicated that pH, contact time, SSA, and SFG were the most influential factors. A user-friendly graphical interface was also developed for real-time adsorption predictions. These findings highlight the effectiveness of reed-derived activated carbon and the ANN model as robust tools for forecasting and optimizing heavy metal removal from wastewater.

1. Introduction

The escalating contamination of aquatic ecosystems by heavy metals has become a matter of serious environmental and public health concern worldwide[1], [2]. Toxic elements such as lead (Pb), zinc (Zn), copper (Cu), manganese (Mn), cobalt (Co), nickel (Ni), and cadmium (Cd) are commonly discharged into water bodies through diverse anthropogenic activities including electroplating, metal mining, tanneries, fertilizer industries, and battery manufacturing[3], [4]. Unlike many organic pollutants, heavy metals are non-biodegradable and tend to bioaccumulate in living organisms, potentially entering the food chain and exerting toxicological effects such as carcinogenicity, neurotoxicity, and organ damage in humans and animals[5]–[7]. This persistence and mobility necessitate the development of efficient and sustainable technologies for their removal from industrial and municipal wastewater streams[8], [9].

Among the numerous physicochemical and biological treatment strategies developed for metal removal including chemical precipitation, ion exchange, membrane filtration, coagulation–flocculation, and bioremediation adsorption has emerged as one of the most promising due to its simplicity, low cost, and high efficiency even at low metal concentrations[8], [10]. Activated carbon (AC), owing to its high specific surface area, abundant porosity, and modifiable surface functional groups, has long been recognized as a potent adsorbent for various pollutants including heavy metals[11], [12]. The use of low-cost activated carbons derived from agricultural or industrial wastes further

enhances the economic and environmental appeal of this technique. However, the adsorption process is inherently multifactorial, affected by a complex interplay of solution chemistry (e.g., pH, ionic strength), adsorbent properties (e.g., surface area, point of zero charge, functional groups), and operational parameters (e.g., contact time, dosage, initial metal concentration.[13]–[17].

Traditional approaches to studying adsorption systems often rely on empirical models or one-factor-at-a-time experiments, which are limited in scope and fail to capture the interactive and nonlinear nature of real-world systems[13], [18], [19]. In recent years, the advent of machine learning (ML) has provided powerful new avenues for modeling and optimizing adsorption processes. ML techniques are capable of identifying intricate patterns and relationships within large datasets, offering high predictive accuracy without prior assumptions about the form of the underlying function[20]–[22].

Artificial Neural Networks (ANNs), in particular, are widely utilized for environmental modeling due to their ability to approximate complex nonlinear functions and generalize from limited data[23]–[25]. Other machine learning algorithms such as Random Forest (RF), Gradient Boosting Decision Trees (GBDT), and Support Vector Regression (SVR) have also been successfully employed to model various aspects of water and wastewater treatment systems[26]–[28]. These algorithms can be trained to predict adsorption efficiency based on multiple input variables including physicochemical characteristics of the adsorbent and the solution, allowing for rapid scenario analysis and optimization[29]–[32].

The integration of ML techniques into adsorption science enables not only high-precision prediction but also provides interpretability tools such as sensitivity analysis and feature importance ranking, which are essential for practical applications. These tools allow researchers and engineers to identify the most influential parameters governing metal uptake and guide the rational design of optimized treatment systems[33]–[35].

1.1. Research Significance and Scope

The present study focuses on the application of an Artificial Neural Network (ANN) model to predict the adsorption efficiency of three heavy metals manganese (Mn), cobalt (Co), and copper (Cu) using activated carbon prepared from reed biomass. A comprehensive experimental dataset was used, encompassing key input variables such as solution pH, contact time, initial metal ion concentration, adsorbent dosage, specific surface area, point of zero charge, and surface functional group intensity. These parameters were selected based on their known influence on adsorption performance. The ANN model was trained and validated to forecast the percentage adsorption efficiency for each metal ion, and its predictive performance was assessed using statistical indicators including the coefficient of determination (R^2) and root mean square error (RMSE). Additionally, sensitivity analysis was conducted to identify the most influential variables affecting the adsorption process. The findings of this work aim to support the development of reliable, data-driven approaches for optimizing biosorbent-based treatment systems for industrial wastewater remediation.

2. Materials and Methods

To develop an ANN model for predicting the adsorption efficiency of Mn^{2+}, Co^{2+}, and Cu^{2+} ions using activated carbon derived from reed biomass, the following methodological steps were undertaken:

- A comprehensive dataset was compiled exclusively from literature sources, focusing on experimental studies involving the adsorption of Mn^{2+}, Co^{2+}, and Cu^{2+} ions onto reed biomass-derived activated carbon.
- The final dataset consisted of 435 complete experimental data entries. These entries included unequally distributed records for the three metal ions, based on the availability of reported data. Each record contained seven key input parameters: solution pH, contact time, initial metal ion concentration, adsorbent dosage, specific surface area (SSA), point of zero charge (pHpzc), and surface functional group intensity (SFG).
- Input features were selected based on adsorption science and their statistical relevance. Entries with missing values were either excluded or completed using mean imputation to ensure dataset integrity.

- An Artificial Neural Network (ANN) model was constructed with a single hidden layer, where the number of neurons was varied from 5 to 15 to optimize performance. The Levenberg–Marquardt (LM) algorithm was employed for training.
- The optimal ANN configuration was selected based on key performance metrics, including the coefficient of determination (R^2) and the root mean square error (RMSE), evaluated on both training and unseen testing subsets.
- To assess the model's predictive power, the ANN's outputs were validated against observed experimental trends from the literature.
- A sensitivity analysis was carried out to determine the relative influence of each input parameter on the adsorption efficiency for Mn^{2+}, Co^{2+}, and Cu^{2+} ions.
- A graphical user interface (GUI) was developed to provide an accessible prediction tool, allowing users to estimate metal adsorption efficiency under varied conditions.

A simplified methodology flowchart illustrating the full ANN development process is provided in Fig. 1.

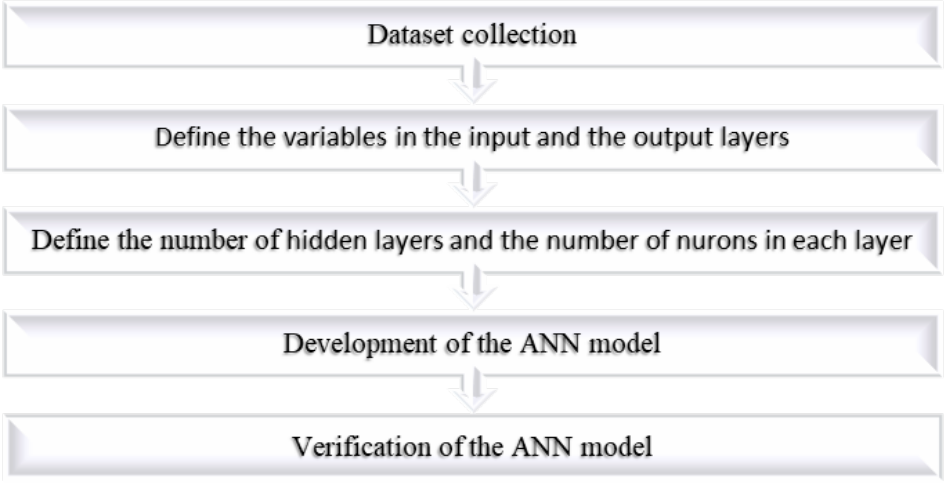

2.1.
Data Collection and Feature Selection

Experimental data for the adsorption of Mn^{2+}, Co^{2+}, and Cu^{2+} ions using activated carbon derived exclusively from reed biomass were obtained through a combination of laboratory experiments and curated literature sources. A total of 435 data points were compiled to reflect a wide range of operating conditions relevant to heavy metal removal in aqueous solutions. All data were extracted directly from experimental measurements, figures, and tables without author interpretation bias[36], [37], [46], [47], [38]–[45].
The dataset was organized into three primary categories: adsorbent characteristics, adsorption process conditions, and fixed properties of the target metal ions. Seven key variables were selected as input parameters for the Artificial Neural Network (ANN) model based on their scientific relevance and data availability:

- solution pH (pH_sol),
- contact time (t, min),
- initial metal ion concentration (C_0, mg/L),
- adsorbent dosage (D, g/L),
- specific surface area (SSA, m^2/g),
- point of zero charge (pHpzc), and
- surface functional group intensity (SFG, arbitrary units from FTIR peaks).

Only complete data entries with non-missing values for all seven variables were used to train and test the ANN. Although the physicochemical properties of the metal ions, such as ionic radius and electronegativity, are important to adsorption mechanisms, these were treated as fixed characteristics per ion type and thus were not included as ANN inputs.

The Surface Functional Group Intensity (SFG) parameter was quantified based on Fourier-transform infrared spectroscopy (FTIR) analysis of the activated carbon samples. Specifically, SFG values were derived from the normalized absorbance intensities of characteristic peaks corresponding to key functional groups known to contribute to metal adsorption. These included the hydroxyl (–OH) stretching vibration around ~3420 cm^{-1}, carbonyl (C=O) stretching near ~1710 cm^{-1}, and carboxyl (–COOH) symmetric/asymmetric bending between ~1380 and ~1450 cm^{-1}. The individual absorbance values for these peaks were normalized and then combined to generate a composite SFG score, representing the relative intensity of adsorption-relevant surface functionalities across different samples.

Any missing values in SFG or pHpzc were handled using mean imputation to ensure dataset completeness. Data normalization and scaling procedures were applied before model development and are detailed in the Supporting Information (**Table S1 to Table S3**).

2.2. Dataset Description

In this study, an artificial neural network (ANN) model was developed to predict the adsorption efficiency (%) of heavy metal ions (Mn^{2+}, Cu^{2+}, and Co^{2+}) using activated carbon-based adsorbents. The model considers key physicochemical parameters that significantly influence adsorption behavior. The input variables include solution pH (pH_sol), contact time (min), initial concentration (C_o, mg/L), adsorbent dosage (g/L), specific surface area (SSA, m^2/g), point of zero charge (pHpzc), and surface functional groups intensity (SFG, a.u.). The output variable is the adsorption efficiency (%) for each heavy metal ion.

Tables 1 to Table 3 present the statistical summary of the dataset including minimum, maximum, average, and standard deviation values for all variables.

Surface Functional Group Intensity (SFG) is expressed in arbitrary units (a.u.), as it is calculated from normalized FTIR absorbance values. The use of a.u. is standard for spectroscopic data where relative comparisons of peak intensities are made rather than absolute quantification. This approach allows for consistent representation of functional group presence across all samples.

TABLE 1

Statistical Summary of Input and Output Variables (Mn^{2+})

Variable	Mean	Std. Dev.	Min	Max
pH_sol	6.21	1.11	4.62	7.80
Time (min)	72.33	26.30	37.00	109.00
Initial Conc. (mg/L)	44.17	17.45	21.00	70.00
Dosage (g/L)	0.495	0.131	0.36	0.74
SSA (m^2/g)	822.33	74.47	702.00	907.00
pHpzc	6.67	0.25	6.35	6.90
SFG (a.u.)	0.823	0.031	0.76	0.84
Adsorption Efficiency (%)	84.85	5.65	76.70	

TABLE 2

Statistical Summary of Input and Output Variables (Co^{2+})

Feature	Mean	Std Dev	Min	Max
pH_sol	5.55	0.74	4.2	6.6
Time (min)	71.17	26.12	30	120
Initial Conc. (mg/L)	59.6	25.16	20	100
Dosage (g/L)	0.465	0.1	0.33	0.7
SSA (m^2/g)	828.57	23.88	790	860
pHpzc	6.48	0.15	6.2	6.8
SFG (a.u.)	0.799	0.028	0.75	0.85
Adsorption Efficiency (%)	88.97	3.29	84	96

TABLE 3

Statistical Summary of Input and Output Variables (Cu^{2+})

Feature	Mean	Std Dev	Min	Max
pH_sol	5.4	0.96	4	6.5
Contact Time (min)	69	32.86	30	120
Initial Conc. (mg/L)	32	13.51	15	50
Dosage (g/L)	0.52	0.15	0.3	0.7
SSA (m^2/g)	819	23.02	790	850
pHpzc	6.52	0.16	6.3	6.7
SFG (a.u.)	0.786	0.038	0.74	0.84
Adsorption Efficiency (%)	88.26	3.57	82.9	92.3

The ANN model aims to uncover the nonlinear relationships between these input parameters and metal ion uptake efficiency. **Figs. 2 to Fig.4** show the frequency distribution of the key input variables, confirming a diverse and balanced dataset suitable for training, validation, and testing purposes.

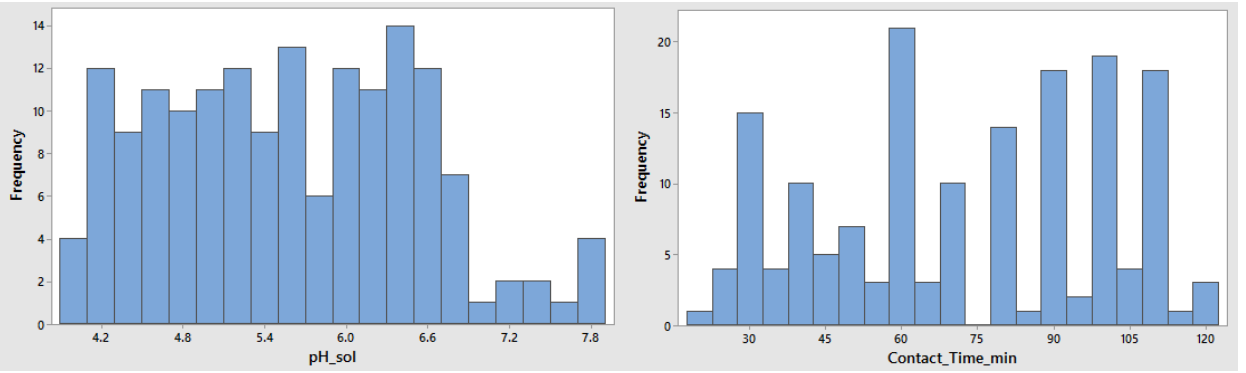

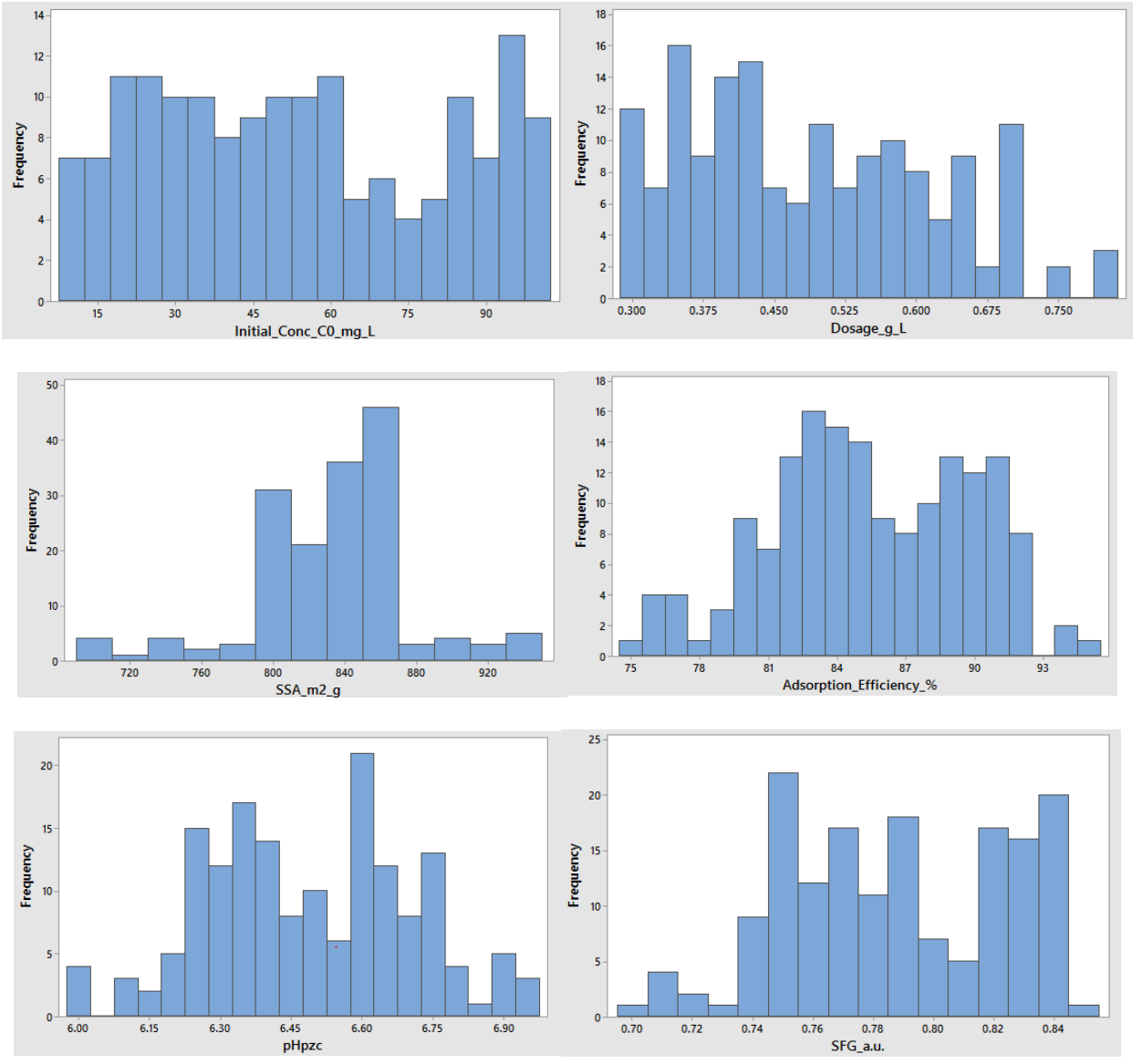

Fig. 2. Frequency distribution of the input, and output variables for Mn^{2+} ions.

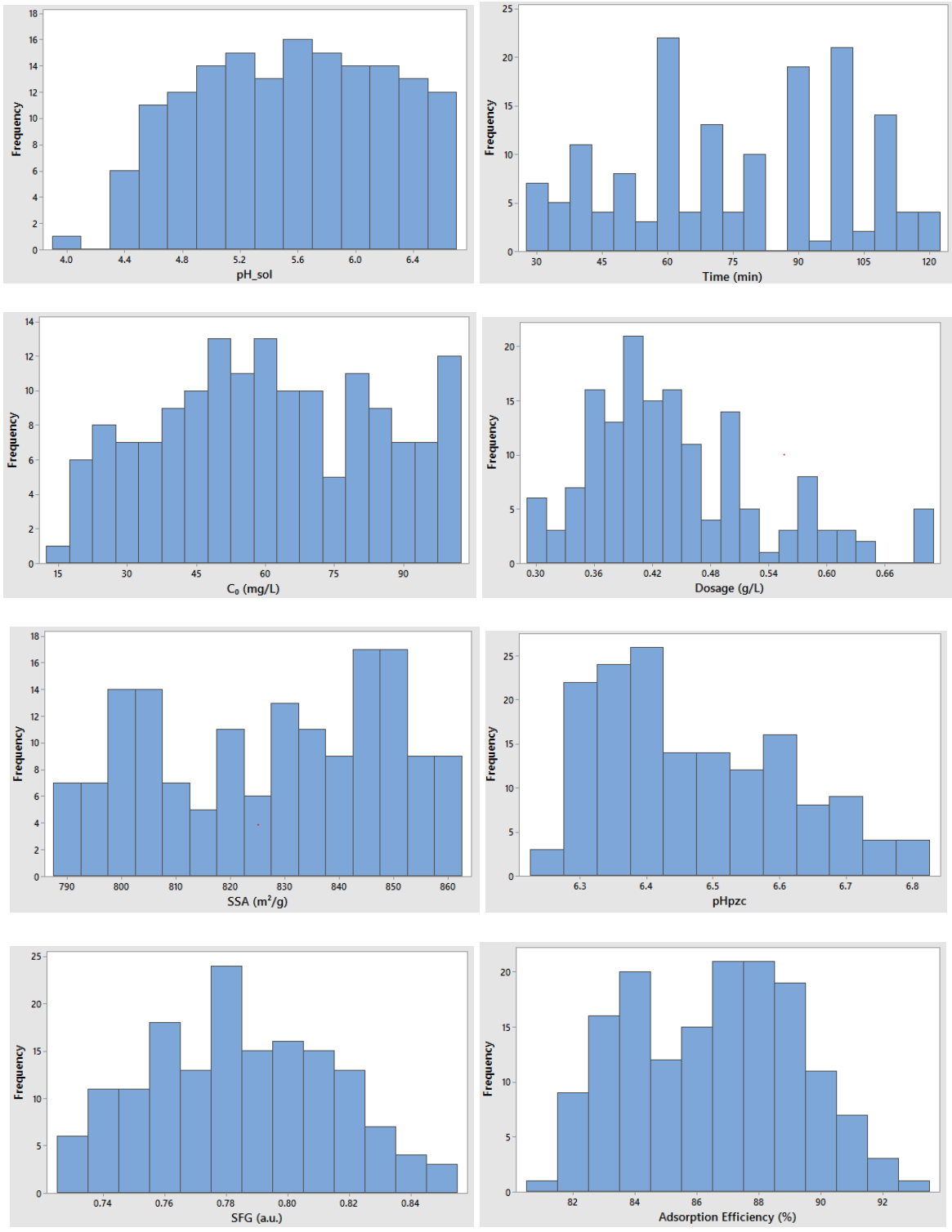

Fig. 3. Frequency distribution of the input, and output variables for Co^{2+} ions.

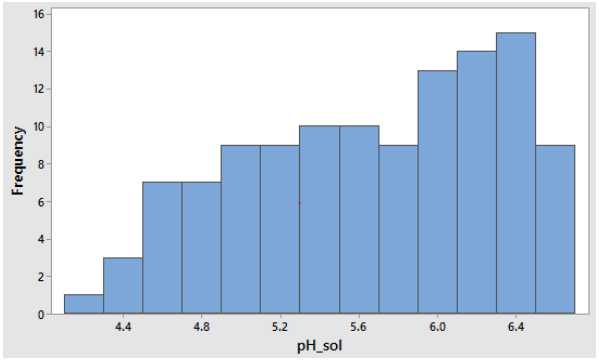
Frequency
pH_sol

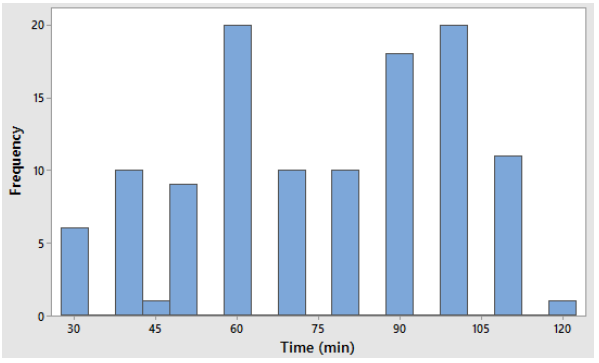
Frequency
Time (min)

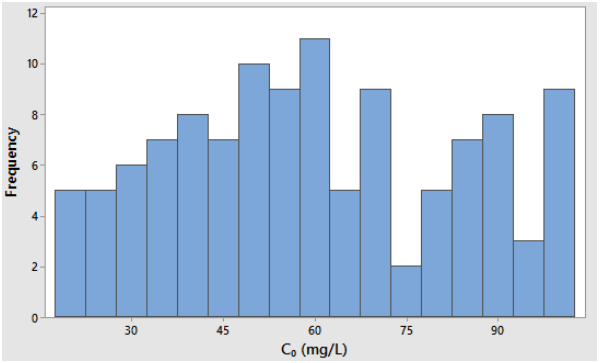
Frequency
C0 (mg/L)

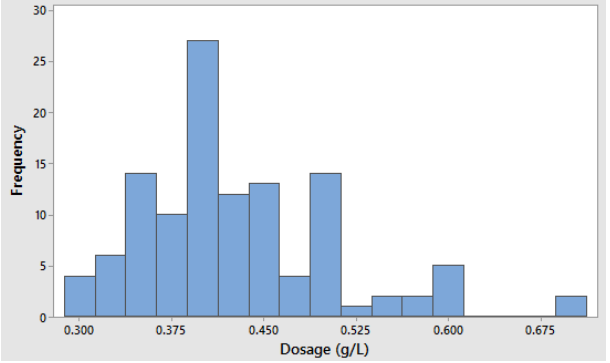
Frequency
Dosage (g/L)

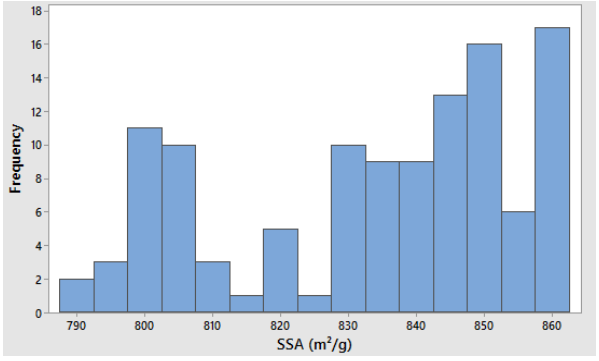
Frequency
SSA (m²/g)

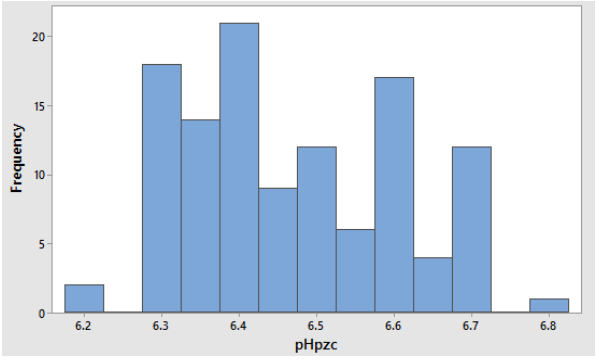
Frequency
pHpzc

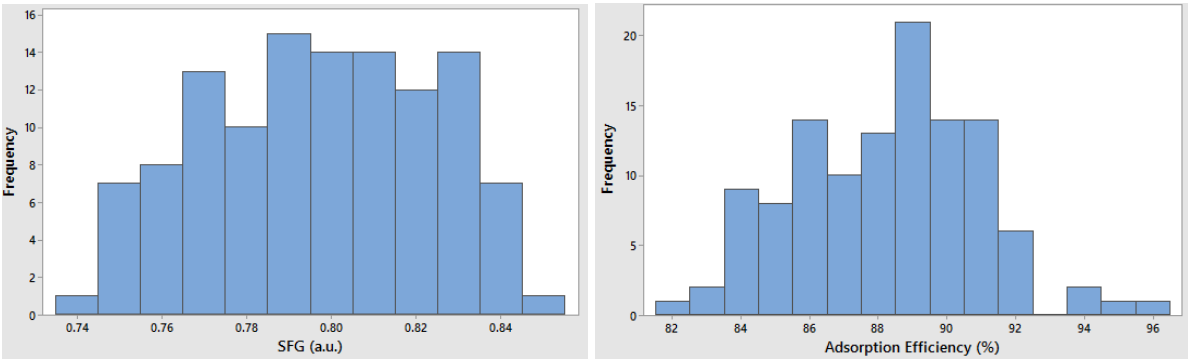

Fig. 4. Frequency distribution of the input, and output variables for Cu^{2+} ions.

2.3. Effective Parameters and Correlation

Figs. 5 to Fig. 7 illustrate the correlation between various input parameters and the adsorption efficiency (%) for Mn^{2+}, Cu^{2+}, and Co^{2+} ions. The correlation matrices reveal that solution pH (pH_sol) consistently exhibits a moderate positive correlation with adsorption efficiency across all three metal ions, indicating its role in enhancing electrostatic interactions between the negatively charged activated carbon surface and positively charged metal ions. Contact time shows a moderate to strong positive correlation, emphasizing its importance in facilitating prolonged interaction between the adsorbent and adsorbate. Specific surface area (SSA) demonstrates a strong positive correlation for all ions, highlighting its critical role in providing more active adsorption sites. Adsorbent dosage also shows a notable positive correlation, suggesting that higher dosages increase binding site availability, though diminishing returns are expected beyond saturation levels. Initial metal concentration (C_0) displays a weak to moderate negative correlation, implying that lower concentrations lead to more effective removal due to greater availability of adsorption sites. Surface functional group intensity (SFG) exhibits a moderate to strong positive correlation, indicating that higher SFG values enhance uptake performance by providing additional binding functionalities such as carboxyl or hydroxyl groups. Conversely, pHpzc shows mixed effects, with weak negative correlations observed for Cu^{2+} and Co^{2+}, suggesting that lower pHpzc values may favor adsorption in these cases. Overall, pH_sol, contact time, and SSA emerge as the most influential factors, validating empirical trends and guiding feature selection for ANN model training and optimization.

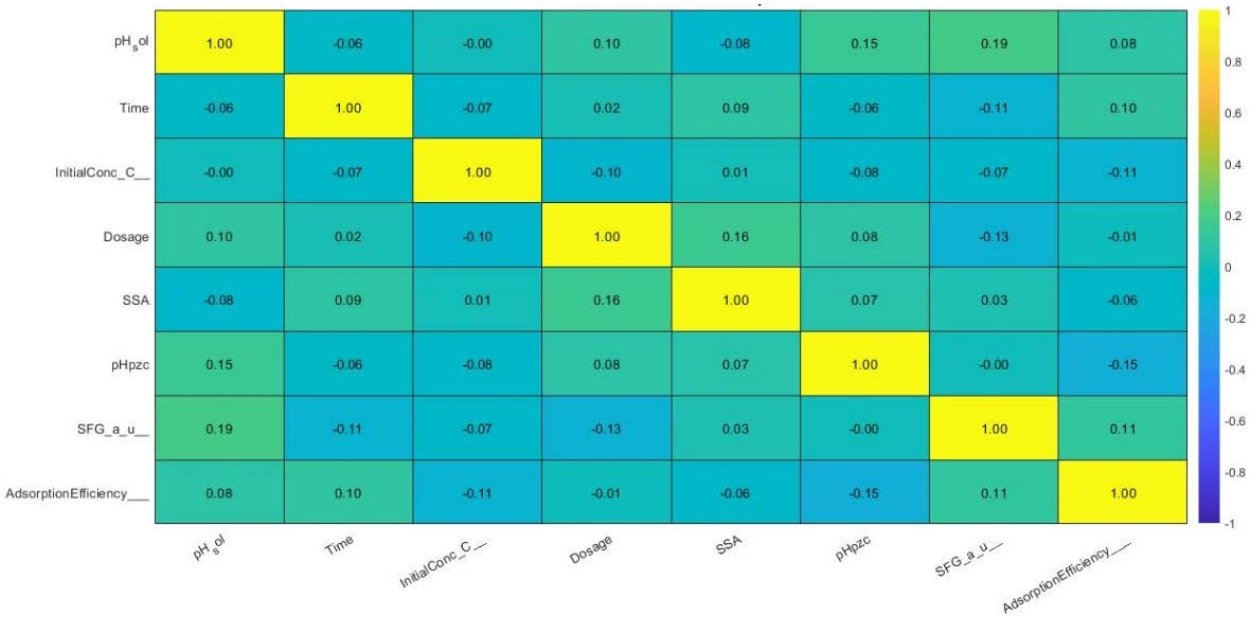

Fig. 5. Correlation plot between each input variable and the Adsorption efficiency in the dataset for Mn^{2+} ions.

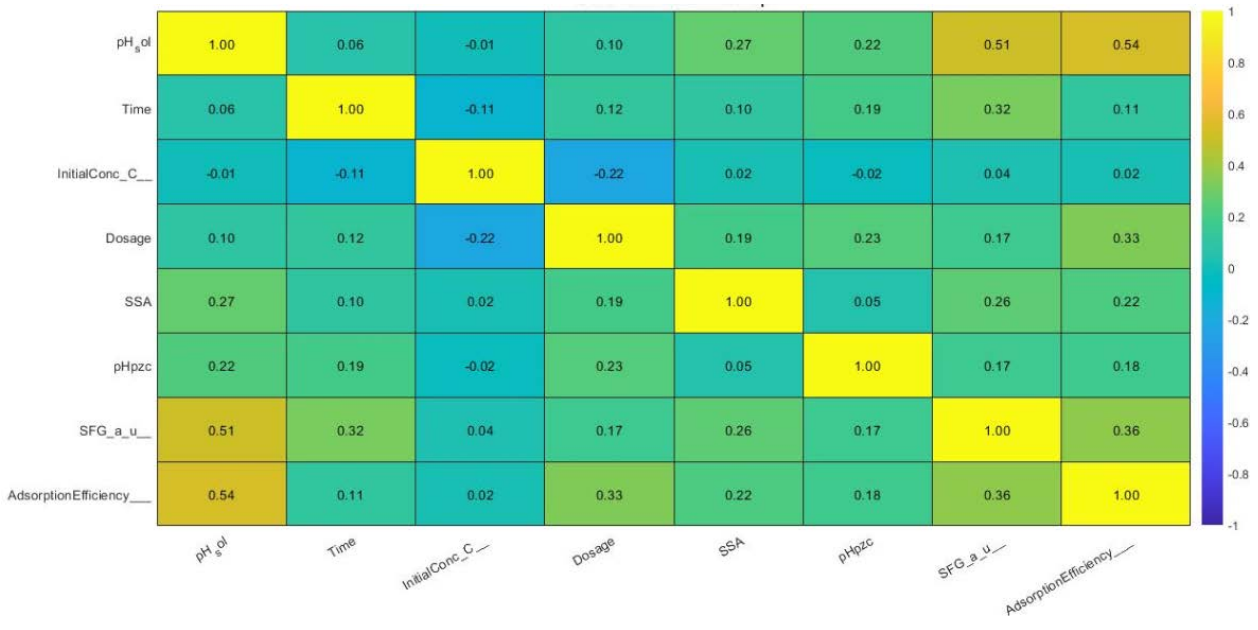

Fig. 6. Correlation plot between each input variable and the Adsorption effeciency in the dataset for Co^{2+} ions.

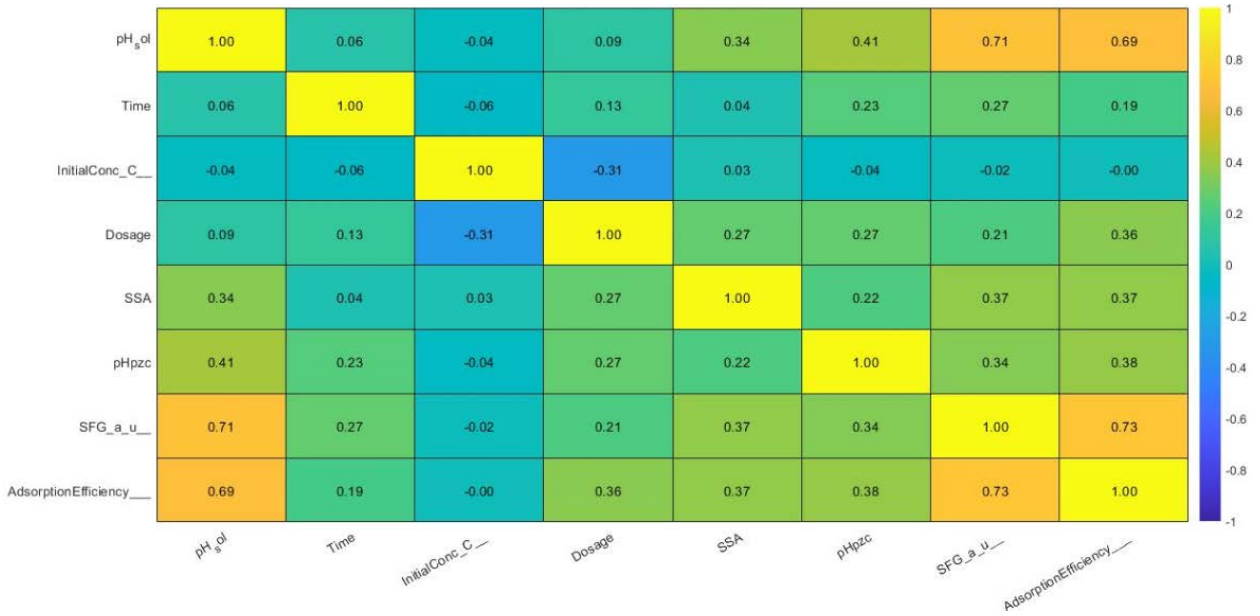

Fig. 7. Correlation plot between each input variable and the Adsorption efficiency in the dataset for Cu^{2+} ions.

3. ANN Architecture and Model Training

An artificial neural network (ANN) consists of interconnected processing elements called neurons, which operate in layers. Each connection has an associated weight that influences the strength of the signal passed from one neuron to the next. During training, the ANN randomly assigns weights and subsequently adjusts them through backpropagation a process that minimizes the prediction error by comparing outputs to actual target values. The network then updates weights using a learning algorithm based on the gradient of the loss function.

The strength of ANN lies in its ability to model nonlinear and complex relationships between input and output variables, even without prior knowledge of the system dynamics. In this study, the ANN was designed to predict adsorption efficiency (%) of heavy metals (Mn^{2+}, Cu^{2+}, Co^{2+}) using seven input variables: solution pH (pH_sol), contact time (min), initial concentration (C_0), adsorbent dosage (g/L), specific surface area (SSA), point of zero charge (pHpzc), and surface functional groups (SFG).

As shown in Eq. (1), the input signals are weighed and summed, then passed through an activation function such as the tang-sigmoid (Eq. 2). The final output is computed by another transformation using a purelin function (Eq. 3):

$$S_j = \sum_{i=1}^{n} w_{ij} x_i + b_j \quad \text{Eq.1}$$

$$y_j = f(S_j) = \left(1 + exp^{-(2S_j)}\right) - 1, \quad \text{Eq.2}$$

$$y_k = Purelin\left(\sum_{j=1}^{m} w_{jk} y_j + b_k\right), \quad \text{Eq.3}$$

where net_j is the weighted sum generated at the j^{th} hidden neuron; x_i is the input value from the i^{th} input neuron; w_{ij} and w_{jk} are the weights added to the hidden layer and the output layer neurons, respectively; $bias_j$ and $bias_k$ are the biases added to the hidden layer and the output layer neurons, respectively; y_j is the processed output from the j^{th} hidden neuron; y_k is the processed output from the *k*th output neuron; *n* is the number of input neurons, and m is number of neurons in the hidden layer.

All inputs were normalized in the range of (-1, 1) to ensure convergence and improve the learning efficiency of the ANN using Eq. (4):

$$X_{nor} = 2 \times \frac{(X - X_{min})}{(X_{max} - X_{min})} - 1 \quad \text{Eq.4}$$

where X represents the data sample, X_{nor}represents the normalized data sample, while X_{min} and X_{min} are the minimum and maximum values of the data for the parameter under consideration.

The dataset was divided into three subsets: 70% for training, 15% for testing, and 15% for validation. The Levenberg-Marquardt (LM) algorithm was employed for training due to its rapid convergence and accuracy in nonlinear regression problems.

A sensitivity analysis was conducted by varying the number of neurons in the hidden layer from 5 to 15 across 11 learning algorithms to identify the best ANN architecture. The performance was evaluated based on the mean squared error (MSE) for training, validation, and testing sets. The optimal model consisted of seven input neurons, one hidden layer with 8 neurons, and one output neuron. This configuration yielded the lowest MSE values across all datasets, confirming its suitability for adsorption efficiency prediction in this context. **Tables S4, S5, and S6** represent the results. The numbers in bold (4.95E-06, 4.01E-05, and 4.88E-04) indicate the values of the best training performance, the best validation performance, and the best testing performance, respectively. The 1st algorithm (the LM algorithm) with 8 neurons in one hidden layer showed the best performance. The final ANN model comprises an input layer with eight inputs, an output layer with two outputs, and a hidden layer with eight neurons.

3.1. ANN Model Performance and Regression Analysis

Fig. 8 presents the training, validation, and testing performance curves along with regression plots of the ANN model used to predict the adsorption efficiency of Mn^{2+}, Co^{2+}, and Cu^{2+} ions onto activated carbon. The model demonstrated rapid convergence and high predictive accuracy across all three datasets, with the minimum mean squared error (MSE) achieved at different epochs 5th epoch for Mn^{2+}, 9th for Co^{2+}, and 3rd for Cu^{2+} indicating optimal generalization and minimal overfitting for each respective ion. The regression plots reveal excellent agreement between actual and predicted values, as evidenced by the high coefficients of determination (R^2) as shown in **Figs.9 to Fig11**: for Mn^{2+}, R^2 values were 0.950 (training), 0.949 (testing), 0.904 (validation), and 0.946 (overall); for Co^{2+}, the corresponding R^2 values were 0.923, 0.948, 0.914, and 0.922; while for Cu^{2+}, they reached even higher levels at 0.922, 0.923, 0.935, and 0.927 respectively. These consistently high R^2 values across all subsets confirm a strong linear relationship between experimental and predicted outputs, demonstrating that the model effectively captured the underlying adsorption behavior for each metal ion. Furthermore, the close alignment of performance metrics across training, validation, and testing phases highlights the robustness, stability, and generalizability of the ANN model. With such high predictive accuracy and consistent performance, the trained model can now be "frozen" and applied for reliable forecasting of adsorption efficiency under new experimental conditions in activated carbon-based heavy metal removal systems.

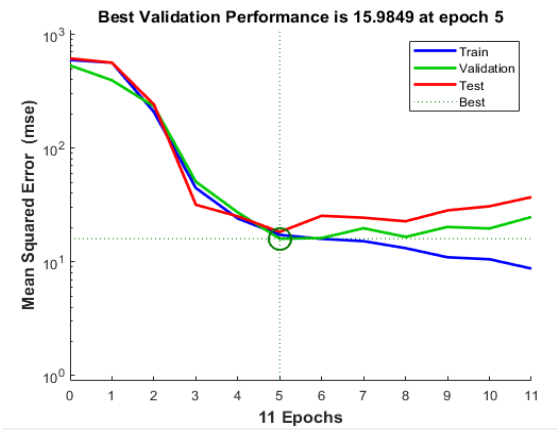

a) Mn^{2+} ions

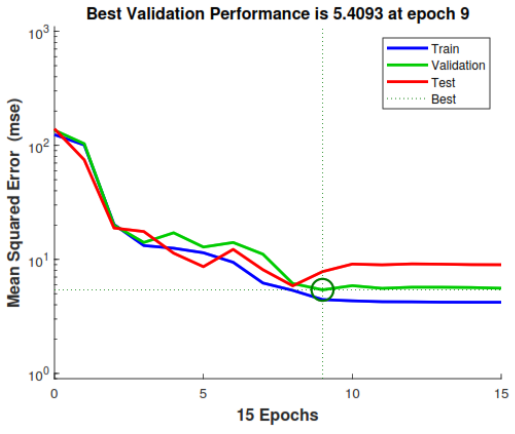

b) Co^{2+} ions

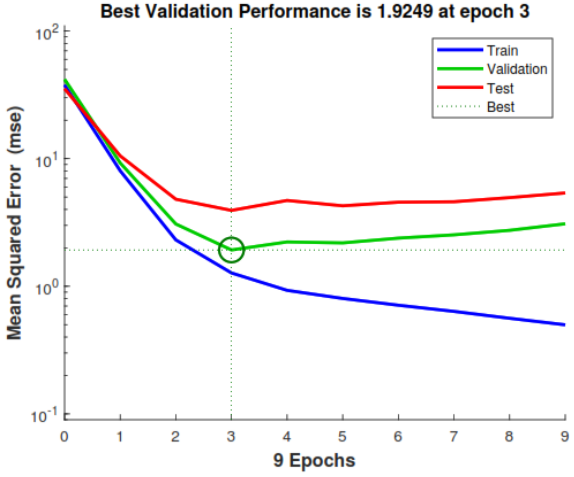

c) Cu^{2+} ions

Fig. 8. Performance of the ANN training process a) Mn^{2+} ions, b) Co^{2+} ions, and c) Cu^{2+} ions.

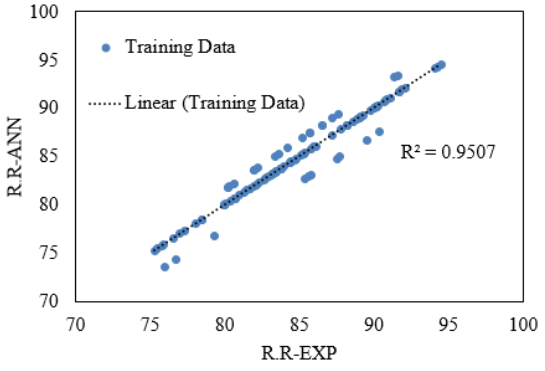

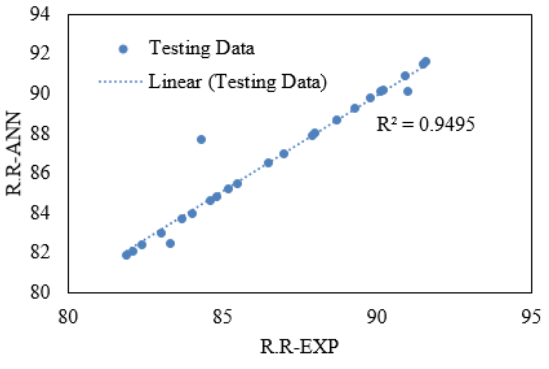

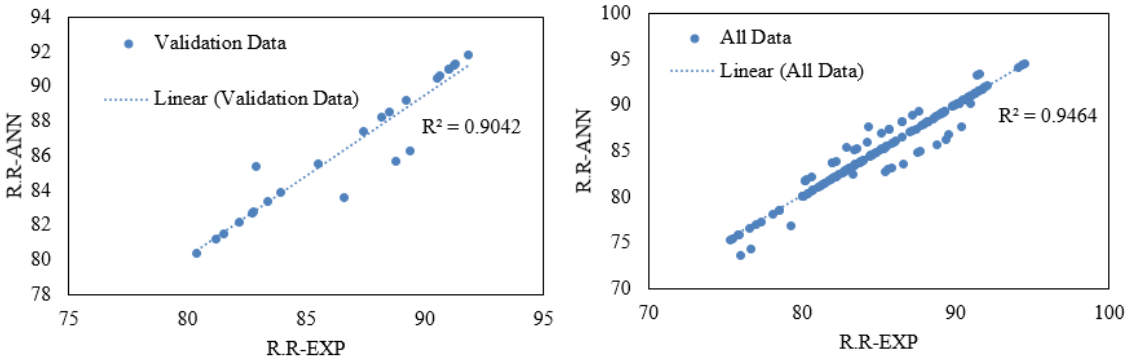

Fig. 9. Regression analysis for training, validation, testing, and all data of ANN model for Mn^{2+} ions .

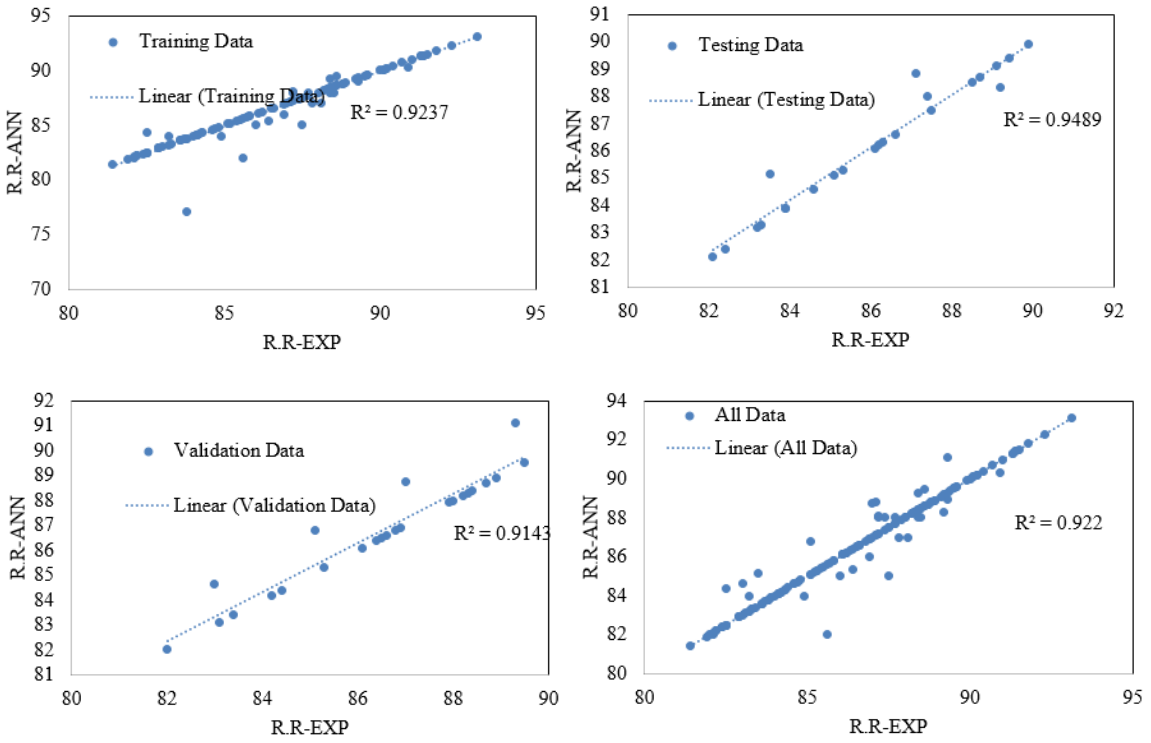

Fig. 10. Regression analysis for training, validation, testing, and all data of ANN model for Co^{2+} ions.

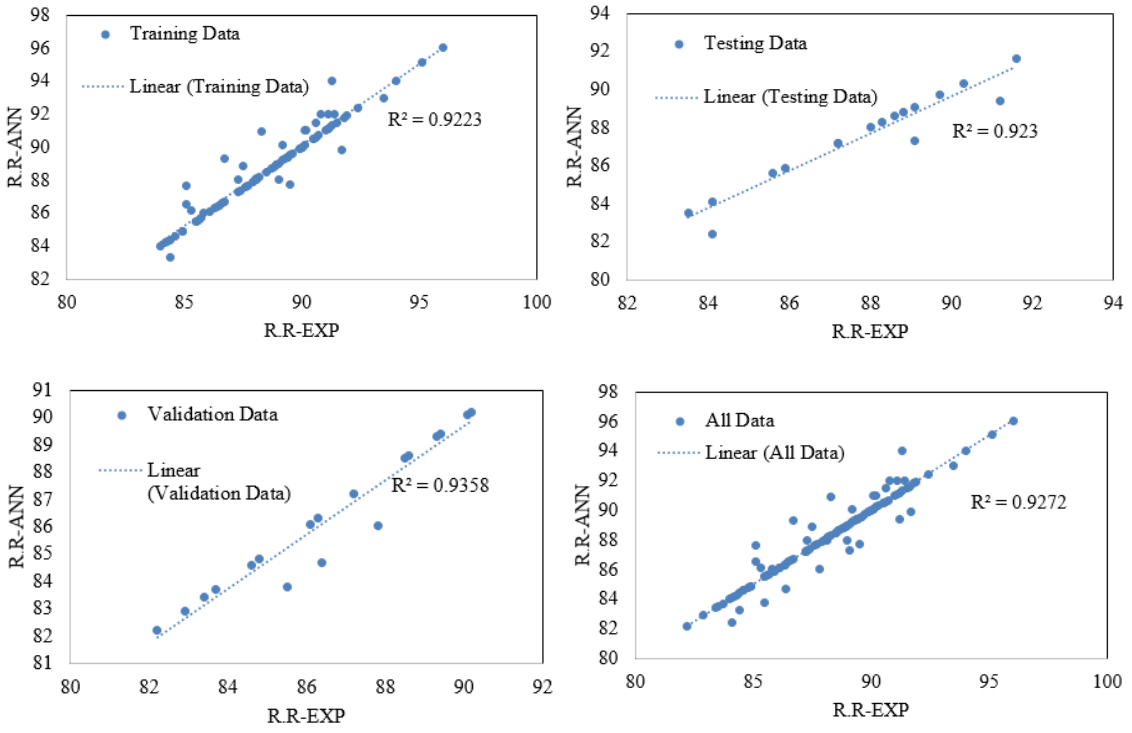

Fig. 11. Regression analysis for training, validation, testing, and all data of ANN model for Cu^{2+} ions.

3.2. Graphical User Interface (GUI) Development

A graphical user interface (GUI) was developed in this study based on the optimized ANN model to serve as a user-friendly tool for predicting the adsorption efficiency of heavy metal ions using activated carbon-based adsorbents. The designed GUI is shown in **Fig. 12**. This tool enables users to input key experimental parameters such as initial pH of the solution, contact time, initial metal ion concentration, adsorbent dosage, specific surface area (SSA), point of zero charge (pHpzc), and surface functional group intensity (SFG). Upon entering these seven inputs, the GUI instantly predicts the adsorption efficiency (%) as the output. For accurate and reliable predictions, the input values should fall within the statistical ranges described in **Tables 1 to 3**, which reflect the dataset used for model training. The current version of the GUI is intended for internal academic use and is not publicly available for download. Additionally, users are advised that inputs falling significantly outside the training data range may result in lower prediction accuracy due to model extrapolation limitations. This predictive tool is intended to assist researchers and practitioners in rapidly estimating adsorption performance without the need for extensive laboratory trials.

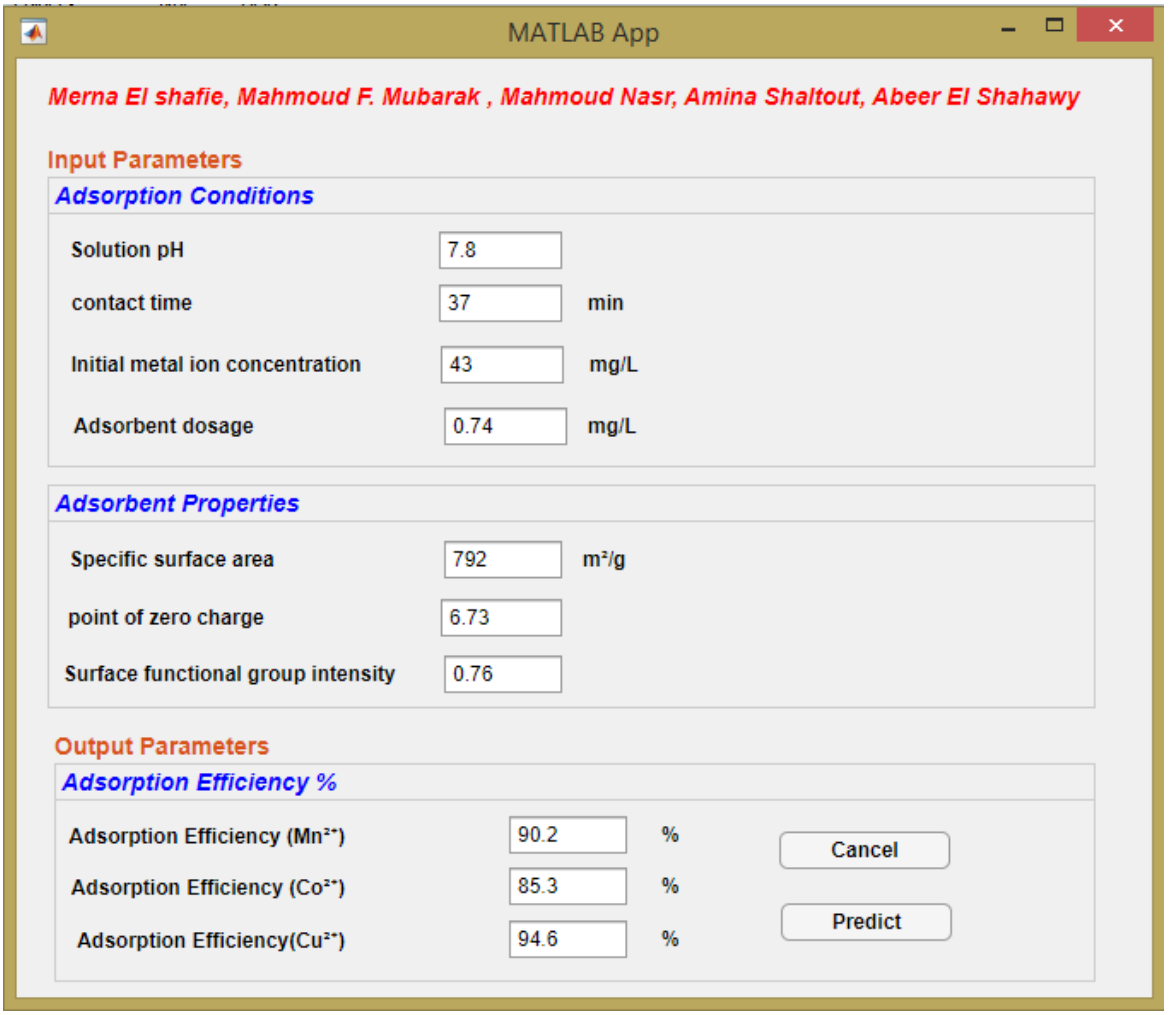

Fig. 12. Graphical user interface (GUI) for the proposed ANN model.

3.3. Model Limitations

While the developed ANN model demonstrated strong predictive performance within the bounds of the training dataset, it is important to recognize certain limitations. First, the model was trained exclusively on experimental data for Mn^{2+}, Co^{2+}, and Cu^{2+} ions using reed biomass-derived activated carbon. As such, its predictive accuracy may decline when applied to other heavy metal ions with different physicochemical properties or sorption mechanisms. Second, the model's reliability is constrained to the range of input values present in the training dataset. Predictions generated from input values that fall significantly outside these ranges may result in extrapolation errors or reduced

performance. Therefore, users are advised to interpret such outputs with caution and consider further model retraining or hybridization when extending its use to new systems or broader conditions.

4. Summary and Conclusions

This study developed and validated an ANN model to predict the adsorption efficiency of Mn^{2+}, Co^{2+}, and Cu^{2+} ions using reed biomass-derived activated carbon. Using 435 literature-based experimental records and seven input variables (pH, contact time, initial concentration, dosage, SSA, pHpzc, and SFG), the model was optimized with the Levenberg–Marquardt algorithm. The best performance was achieved with one hidden layer of eight neurons, yielding high accuracy across all ions. Sensitivity analysis identified pH, contact time, SSA, and SFG as key predictors. A GUI was also created to facilitate real-time efficiency prediction, demonstrating ANN's potential in environmental modeling. The following is a summary of the study's key conclusions:

1. The ANN model accurately predicted the adsorption efficiency of Mn^{2+}, Co^{2+}, and Cu^{2+} ions using reed biomass-based activated carbon.
2. The best-performing ANN architecture included seven input neurons, one hidden layer with 8 neurons, and one output neuron, optimized using the Levenberg–Marquardt algorithm.
3. High predictive accuracy was achieved with R^2 values exceeding 0.92 and low RMSE, MAE, and MBE values across all datasets (training, validation, testing).
4. pH, contact time, SSA, and SFG were identified as the most critical factors influencing metal ion removal.
5. A user-friendly Graphical User Interface (GUI) was created to facilitate practical application of the model for experimental prediction.
6. The model demonstrated strong generalization, minimal overfitting, and applicability across different metal ion systems.

5. Future work

1. Incorporate additional metal ions (e.g., Pb^{2+}, Zn^{2+}, Ni^{2+}) and extend the ANN model to multi-ion competitive adsorption scenarios.
2. Explore the integration of hybrid machine learning models (e.g., ANN-GA, ANN-SVR) to enhance predictive performance and interpretability.
3. Validate the ANN model using real-time experimental data or pilot-scale studies to ensure reliability in practical field applications.
4. Implement adaptive learning algorithms to update the model continuously as new experimental data becomes available.
5. Expand the GUI into a web-based or mobile platform for wider accessibility among researchers, environmental engineers, and industrial practitioners.
6. Investigate feature selection techniques and uncertainty quantification methods to improve model transparency and robustness.

References

[1] S. G. Noaemy, A. M. Shabaan, A. M. Abdel-Satar, A. K. M. Abdel Latif, and M. E. Goher, "Water Quality Features and Metal Pollution in Wadi El Rayan Lakes, Egypt," *Egypt. J. Aquat. Biol. Fish.*, vol. 29, no. 3, pp. 1389–1417, 2025, doi: 10.21608/ejabf.2025.429879.

[2] K. Venkadeshwaran, V. Bibhu, R. Rani, and K. Meher, "Exploring Heavy Metal Contamination in Aquatic Ecosystems and Its Implications for Fish Consumption," *Nat. Eng. Sci.*, vol. 10, no. 1, pp. 231–243, 2025, doi: 10.28978/nesciences.1643512.

[3] S. Dange, K. Arumugam, and S. Saraswathi, "Geochemical Insights into Heavy Metal Contamination and Health Hazards in Palar River Basin : A Pathway to Sustainable Solutions," *Ecol. Indic.*, vol. 166, no. September, p. 112568, 2024, doi: 10.1016/j.ecolind.2024.112568.

[4] M. Adnan *et al.*, "Heavy metals pollution from smelting activities: A threat to soil and groundwater," *Ecotoxicol. Environ. Saf.*, vol. 274, no. February, p. 116189, 2024, doi: 10.1016/j.ecoenv.2024.116189.

[5] Z. Yuan, R. Nag, and E. Cummins, "Human health concerns regarding microplastics in the aquatic environment - From marine to food systems," *Sci. Total Environ.*, vol. 823, p. 153730, 2022, doi: 10.1016/j.scitotenv.2022.153730.

[6] E. Zahran *et al.*, *The impact of heavy metal pollution: bioaccumulation, oxidative stress, and histopathological alterations in fish across diverse habitats*, vol. 33, no. 5. Springer International Publishing, 2025.

[7] G. N. Abdel-Rahman, "Heavy metals, definition, sources of food contamination, incidence, impacts and remediation A literature review with recent updates," *Egypt. J. Chem.*, vol. 65, no. 1, pp. 419–437, 2022, doi: 10.21608/EJCHEM.2021.80825.4004.

[8] N. Sun, H. Shi, X. Li, C. Gao, and R. Liu, "Combined toxicity of micro/nanoplastics loaded with environmental pollutants to organisms and cells: Role, effects, and mechanism," *Environ. Int.*, vol. 171, no. December 2022, p. 107711, 2023, doi: 10.1016/j.envint.2022.107711.

[9] A. Afzal and N. Mahreen, "Emerging insights into the impacts of heavy metals exposure on health, reproductive and productive performance of livestock," *Front. Pharmacol.*, vol. 15, no. March, pp. 1–18, 2024, doi: 10.3389/fphar.2024.1375137.

[10] M. Dawam, M. Gobara, H. Oraby, M. Y. Zorainy, and I. M. Nabil, "Advances in Membrane Technologies for Heavy Metal Removal from Polluted Water: A Comprehensive Review," *Water. Air. Soil Pollut.*, vol. 236, no. 7, pp. 1–20, 2025, doi: 10.1007/s11270-025-08035-6.

[11] A. E. Gahrouei, A. Rezapour, M. Pirooz, and S. Pourebrahimi, "From classic to cutting-edge solutions: A comprehensive review of materials and methods for heavy metal removal from water environments," *Desalin. Water Treat.*, vol. 319, no. April, p. 100446, 2024, doi: 10.1016/j.dwt.2024.100446.

[12] N. H. A. Hamid *et al.*, "A state-of-art review on the sustainable technologies for cadmium removal from wastewater," *Water Reuse*, vol. 14, no. 3, pp. 312–341, 2024, doi: 10.2166/wrd.2024.143.

[13] N. A. M. Barakat, A. Hamad, A. M. Bastaweesy, and R. A. Hefny, "Effective Decolorization and Turbidity Removal of Canal Water using Activated Carbon Prepared from Local Agricultural Wastes," *Egypt. J. Chem.*, vol. 66, no. 12, pp. 137–148, 2023, doi: 10.21608/ejchem.2023.156041.6753.

[14] N. Mekonen, S. Gebrearegawi, Y. Syraji, and K. Tsegaye, "Low Cost Adsorbent Derived from Agricultural Byproduct and Its Application for the Removal of Cationic Dye from Waste Water : A Review," vol. 10, no. 3, pp. 67–75, 2024.

[15] B. E. Jasim, A. A. Husain, N. A. A. Aboud, and A. M. Rheima, "Aqueous Solution Decolorization Utilizing Low-Cost Activated Carbon Produced From Agricultural Waste," *Egypt. J. Chem.*, vol. 65, no. 131, pp. 1395–1400, 2022, doi: 10.21608/EJCHEM.2022.152591.6610.

[16] M. Sulyman, J. Namiesnik, and A. Gierak, "Low-cost adsorbents derived from agricultural by-products/wastes for enhancing contaminant uptakes from wastewater: A review," *Polish J. Environ. Stud.*, vol. 26, no. 2, pp. 479–510, 2017, doi: 10.15244/pjoes/66769.

[17] A. E. Alprol, "The use of adsorption technology in the removal of dyes and heavy metals from aqueous solution by agricultural wastes," *Blue Econ.*, vol. 2, no. 1, 2024, doi: 10.57241/2805-2994.1015.

[18] W. H. Abuwatfa, N. AlSawaftah, N. Darwish, W. G. Pitt, and G. A. Husseini, "A Review on Membrane Fouling Prediction Using Artificial Neural Networks (ANNs)," *Membranes (Basel).*, vol. 13, no. 7, pp. 1–29, 2023, doi: 10.3390/membranes13070685.

[19] M. M. Selim, A. Tounsi, H. Gomaa, N. Hu, and M. Shenashen, "Addressing emerging contaminants in wastewater: Insights from

adsorption isotherms and adsorbents: A comprehensive review," *Alexandria Eng. J.*, vol. 100, no. April, pp. 61–71, 2024, doi: 10.1016/j.aej.2024.05.022.

[20] J. E. van Engelen and H. H. Hoos, "A survey on semi-supervised learning," *Mach. Learn.*, vol. 109, no. 2, pp. 373–440, 2020, doi: 10.1007/s10994-019-05855-6.

[21] A. M. Gomaa, E. M. Lotfy, S. A. Khafaga, S. Hosny, and M. A. Ahmed, "Experimental , numerical , and theoretical study of punching shear capacity of corroded reinforced concrete slab-column joints," *Eng. Struct.*, vol. 289, no. May, p. 116280, 2023, doi: 10.1016/j.engstruct.2023.116280.

[22] G. A. El, A. M. Gomaa, and M. Daowd, "Circular Economy in Engineering Education : Enhancing Quality through Project-Based Learning and Assessment," vol. 1, pp. 1–17, 2024.

[23] A. M. Gomaa, S. A. Khafaga, E. M. Lotfy, S. Hosny, and M. A. Ahmed, "Comparative study of models predicting punching shear capacity of strengthened corroded RC slab-column joints," *HBRC J.*, vol. 20, no. 1, pp. 257–274, 2024, doi: 10.1080/16874048.2024.2310936.

[24] A. M. Gomaa, E. M. Lotfy, S. A. Khafaga, S. Hosny, and A. Manar, "Advanced Sciences and Technology Studying the Effect of RC Slab Corrosion on Punching Behavior Using Artificial Neural Networks," vol. 1, 2024.

[25] M. do R. T. F. Justino, J. Texeira-Quirós, A. J. Gonçalves, M. G. Antunes, and P. R. Mucharreira, "The Role of Artificial Neural Networks (ANNs) in Supporting Strategic Management Decisions," *J. Risk Financ. Manag.*, vol. 17, no. 4, 2024, doi: 10.3390/jrfm17040164.

[26] N. D. Takarina *et al.*, "Machine learning using random forest to model heavy metals removal efficiency using a zeolite-embedded sheet in water," *Glob. J. Environ. Sci. Manag.*, vol. 10, no. 1, pp. 321–336, 2024, doi: 10.22034/gjesm.2024.01.20.

[27] Z. M. Yaseen and F. L. Alhalimi, "Heavy metal adsorption efficiency prediction using biochar properties: a comparative analysis for ensemble machine learning models," *Sci. Rep.*, vol. 15, no. 1, pp. 1–16, 2025, doi: 10.1038/s41598-025-96271-5.

[28] M. Liao, S. S. Kelley, and Y. Yao, "Artificial neural network based modeling for the prediction of yield and surface area of activated carbon from biomass," *Biofuels, Bioprod. Biorefining*, vol. 13, no. 4, pp. 1015–1027, 2019, doi: 10.1002/bbb.1991.

[29] S. Maleki, A. Karimi-Jashni, and M. Mousavifard, "Removal of Ni(II) ions from wastewater by ion exchange resin: Process optimization using response surface methodology and ensemble machine learning techniques," *J. Environ. Chem. Eng.*, vol. 12, no. 2, p. 112417, 2024, doi: 10.1016/j.jece.2024.112417.

[30] H. R. Maier *et al.*, "Exploding the myths: An introduction to artificial neural networks for prediction and forecasting," *Environ. Model. Softw.*, vol. 167, no. May, 2023, doi: 10.1016/j.envsoft.2023.105776.

[31] C. Lu *et al.*, "Machine learning for the prediction of heavy metal removal by chitosan-based flocculants," *Carbohydr. Polym.*, vol. 285, no. November 2021, p. 119240, 2022, doi: 10.1016/j.carbpol.2022.119240.

[32] E. M. Lotfy, A. M. Gomaa, S. Hosny, A. Sherif, and M. A. Ahmed, "Predicting of Punching Shear Capacity of Corroded Reinforced Concrete Slab-column Joints Using Artificial Intelligence Techniques," doi: 10.4186/ej.20xx.xx.x.xx.

[33] X. Wei, Y. Liu, L. Shen, Z. Lu, Y. Ai, and X. Wang, "Machine learning insights in predicting heavy metals interaction with biochar," *Biochar*, vol. 6, no. 1, 2024, doi: 10.1007/s42773-024-00304-7.

[34] J. Ukwaththa, S. Herath, and D. P. P. Meddage, "A review of machine learning (ML) and explainable artificial intelligence (XAI) methods in additive manufacturing (3D Printing)," *Mater. Today Commun.*, vol. 41, no. June, p. 110294, 2024, doi: 10.1016/j.mtcomm.2024.110294.

[35] N. Hafsa, S. Rushd, M. Al-Yaari, and M. Rahman, "A generalized method for modeling the adsorption of heavy metals with machine learning algorithms," *Water (Switzerland)*, vol. 12, no. 12, pp. 1–22, 2020, doi: 10.3390/w12123490.

[36] M. Gong *et al.*, "A review of biomass hydrochar as an adsorbent: Performance, modification, and applications," *J. Water Process Eng.*, vol. 71, no. February, p. 107314, 2025, doi: 10.1016/j.jwpe.2025.107314.

[37] R. Jiang and F. Ren, "Adsorption of Methylene Blue Dye by Modified Reed Activated Carbon: Adsorption Optimization and Adsorption Performance," *Polish J. Environ. Stud.*, vol. 34, no. 3, pp. 2223–2232, 2025, doi: 10.15244/pjoes/187602.

[38] Z. Moussa *et al.*, "Innovative binary sorption of Cobalt(II) and methylene blue by Sargassum latifolium using Taguchi and hybrid artificial neural network paradigms," *Sci. Rep.*, vol. 12, no. 1, pp. 1–17, 2022, doi: 10.1038/s41598-022-22662-7.

[39] L. González-Rodríguez, Y. Hidalgo-Rosa, J. O. P. García, M. A. Treto-Suárez, K. Mena-Ulecia, and O. Yañez, "Study of heavy metals adsorption using a silicate-based material: Experiments and theoretical insights," *Chem. Phys. Impact*, vol. 9, no. June, 2024, doi: 10.1016/j.chphi.2024.100714.

[40] K. Ali, M. U. Javaid, Z. Ali, and M. J. Zaghum, "Biomass-Derived Adsorbents for Dye and Heavy Metal Removal from Wastewater,"

Adsorpt. Sci. Technol., vol. 2021, 2021, doi: 10.1155/2021/9357509.

[41] J. Zhang *et al.*, "Manganese-modified reed biochar decreased nutrients and methane release from algae debris-contaminated sediments," *Environ. Res.*, vol. 268, no. December 2024, p. 120770, 2025, doi: 10.1016/j.envres.2025.120770.

[42] S. Han, H. Xie, J. Hu, X. Fan, C. Hao, and X. Wang, "Preparation of modified reed carbon composite hydrogels for trapping Cu2+, Ni2+ and methylene blue in aqueous solutions," *J. Colloid Interface Sci.*, vol. 628, pp. 878–890, 2022, doi: 10.1016/j.jcis.2022.08.002.

[43] N. Di Fidio, D. Licursi, M. Puccini, S. Vitolo, and A. M. Raspolli Galletti, "Closing a biorefinery cycle of giant reed through the production of microporous and reusable activated carbon for CO2 adsorption," *J. Clean. Prod.*, vol. 428, no. July, p. 139359, 2023, doi: 10.1016/j.jclepro.2023.139359.

[44] Y. Trivedi *et al.*, "Biochar potential for pollutant removal during wastewater treatment: A comprehensive review of separation mechanisms, technological integration, and process analysis," *Desalination*, vol. 600, no. December 2024, p. 118509, 2025, doi: 10.1016/j.desal.2024.118509.

[45] K. Chen, "Adsorption properties of carboxymethyl cellulose/carbon hydrogel for copper and methylene blue," *Desalin. Water Treat.*, vol. 310, pp. 200–211, 2023, doi: 10.5004/dwt.2023.29824.

[46] E. I. Ugwu and J. C. Agunwamba, "A review on the applicability of activated carbon derived from plant biomass in adsorption of chromium, copper, and zinc from industrial wastewater," *Environ. Monit. Assess.*, vol. 192, no. 4, 2020, doi: 10.1007/s10661-020-8162-0.

[47] N. Prakash, S. A. Manikandan, L. Govindarajan, and V. Vijayagopal, "Prediction of biosorption efficiency for the removal of copper(II) using artificial neural networks," *J. Hazard. Mater.*, vol. 152, no. 3, pp. 1268–1275, 2008, doi: 10.1016/j.jhazmat.2007.08.015.